Journal of Plant Physiology 244 (2020) 153060

Contents lists available at ScienceDirect

Journal of Plant Physiology

journal homepage: www.elsevier.com/locate/jplph

The diffusive injection micropipette (DIMP)

Alexander H. Howell, Winfried S. Peters, Michael Knoblauch*

School of Biological Sciences, Washington State University, Pullman, WA, 99164, USA

ARTICLE INFO

Keywords:
Cytoplasmic streaming
Fluorescent probe
Fluorophore
Microinjection
Nicotiana
Trichome

ABSTRACT

The microinjection of fluorescent probes into live cells is an essential component in the toolbox of modern cell biology. Microinjection techniques include the penetration of the plasma membrane and, if present, the cell wall with micropipettes, and the application of pressure or electrical currents to drive the micropipette contents into the cell. These procedures interfere with cellular functions and therefore may induce artifacts. We designed the diffusive injection micropipette (DIMP) that avoids most of the possible artifacts due to the drastically reduced volume of its fluid contents and the utilization of diffusion for cargo delivery into the target cell. DIMPs were successfully tested in plant, fungal, and animal cells. Using the continuity of cytoplasmic dynamics over ten minutes after impalement of *Nicotiana* trichome cells as a criterion for non-invasiveness, we found DIMPs significantly less disruptive than conventional pressure microinjection. The design of DIMPs abolishes major sources of artifacts that cannot be avoided by other microinjection techniques. Moreover, DIMPs are inexpensive, easy to produce, and can be applied without specific equipment other than a micromanipulator. With these features, DIMPs may become the tool of choice for studies that require the least invasive delivery possible of materials into live cells.

1. Introduction

Modern cell biology relies on the high-resolution imaging of intracellular structures and processes, often utilizing fluorescent probes to reveal the three-dimensional organization of live cells and their dynamics (Sanderson et al., 2014; Stockert and Blázquez-Castro, 2017). Membrane-impermeant fluorophores are particularly powerful tools. Once such a probe is located inside of the plasma membrane, its movement within and between symplasmically connected cells can be monitored directly or after local abolishment of the fluorescence signal by photobleaching (Oparka et al., 2005).

Obviously, the fluorophore should be introduced into the cells by non-invasive methods, to minimize loading-induced artifacts. The least invasive loading techniques utilize fluorogenic substrates that readily diffuse into cells where they yield impermeant fluorescent products following unspecific enzymatic modification. For instance, the membrane-permeant carboxyfluorescein diacetate (CFDA), which is cleaved in the cytosol yielding the impermeant carboxyfluorescein (CF), has been applied to demonstrate cytoplasmic continuity between cells growing in tissue culture (Baron-Epel et al., 1988), to quantify cell-to-cell diffusion in the *Arabidopsis* root meristem (Rutschow et al., 2011), to monitor symplasmic phloem unloading (Oparka et al., 1994; Ross-Elliott et al., 2017), and to visualize mass flow in sieve tubes of plants (Knoblauch and van Bel, 1998) and brown algae (Knoblauch et al., 2016a). Unfortunately, the number of fluorogenic substrates for use in live tissue is limited and the available range of molecular weights is small, resulting in similar behavior of the fluorophores (Wright et al., 1996; Wright and Oparka, 1996). In some cases, the dependence on cellular enzymes for the liberation of the fluorophore can be avoided by using caged fluorophores. An example is fluorescein bis-(5-carboxymethoxy-2-nitrobenzyl) ether (CMNB-F), which diffuses freely into cells where the membrane-impermeant fluorophore fluorescein can be released by UV irradiation (Martens et al., 2004). Again, the available variety of membrane-permeant caged fluorophores is limited, and the generation of toxic byproducts of photoactivation is an additional potential problem (Mitchison et al., 1998).

Another non-invasive way of loading live cells with fluorescent probes is having the cells produce the probes themselves. The advent of the green fluorescent protein (GFP) in the 1990s has revolutionized the study of intracellular transport (Brandizzi et al., 2002), and new types of fluorescent proteins for diverse applications in various cells are being added to our methodological arsenal ever since (Adam, 2014; Enterina et al., 2015; Rodriguez et al., 2017; Sanford and Palmer, 2017; Walia et al., 2018). Genes encoding fluorescent proteins can be expressed in transformed organisms under the control of universal or cell type-specific promoters, or as fusions with target proteins of interest (Oparka

* Corresponding author at: 100 Dairy Road, Eastlick Hall G81, Washington State University, Pullman, 99164, USA.
E-mail addresses: alexander.howell@wsu.edu (A.H. Howell), petersw@pfw.edu (W.S. Peters), knoblauch@wsu.edu (M. Knoblauch).

https://doi.org/10.1016/j.jplph.2019.153060
Received 3 September 2019; Received in revised form 11 October 2019; Accepted 15 October 2019
Available online 01 November 2019

et al., 2005). Despite the versatility of currently available fluorescent proteins, the necessity of time-consuming genetic transformation of the study organism before a protein can be observed is a disadvantage, especially for exploratory or comparative studies in species for which no routine molecular protocols have been established. Moreover, the sizes of fluorescent protein molecules are beyond the size exclusion limit of non-dilated plasmodesmata in many tissues (800–1200 Da; Lucas and Lee, 2004), which may limit their usefulness for the study of symplasmic transport in these systems.

A third but more invasive method of delivering fluorophores into cells is microinjection. Cells are impaled with pointed micropipettes made from glass capillaries that have been filled with the desired cargo. If the cargo consists of small, charged molecules or ions, it can be driven into the cell by electrical currents (iontophoresis). In most cases, however, hydrostatic pressure has to be applied to the micropipette's contents to overcome the friction in the pipette tip and, in plants, fungi, and bacteria, the significant intracellular hydrostatic pressure (Oparka et al., 2005; Knoblauch, 2001). Micropipettes for pressure injection resemble pressure-microprobes for turgor measurement (Green, 1968; Zimmermann and Steudle, 1979; Tomos and Leigh, 1999), and pressure-microprobe setups are readily modified for microinjection experiments (Oparka et al., 1991; Kempers and van Bel, 1997). Consequently, both methods have similar practical difficulties. In walled cells under intracellular pressure the main problem is the maintenance of turgor during the experiment. This is essential in experiments addressing symplasmic continuity in plants, as plasmodesmata respond to wounding and the resulting turgor shifts by changing their size exclusion limits (Oparka and Prior, 1992; Storms et al., 1998; Radford and White, 2001). Similarly, osmotic shock can trigger the closure of septal pores in ascomycetes (Maruyama et al., 2005). The three main factors responsible for artificial turgor shifts are first, leakage at the point of micropipette insertion; this effect can be avoided to some degree depending on the skills and experience of the experimenter. Second, due to the pressure difference between a turgescent cell and the filling of the micropipette, cellular fluid is driven into the pipette at the time of impalement. This effect can be reduced by prepressurizing the micropipette, but the resulting leakage from the pipette tip before impalement can have unacceptable consequences, especially if the cargo includes fluorophores intended for labeling intracellular compartments specifically. Third, while the compressibility of the fluid in the micropipette is small, the volumes of the available systems are huge compared to that of the impaled cell. Thus, fluid compression in the pipette at the time of impalement can lead to significant turgor shifts in the cell (Knoblauch et al., 2014). For these reasons, the delivery of fluorescent probes to cells by microinjection must be considered a more invasive and therefore less suitable method compared to the diffusive loading of fluorogenic substrates or the expression of fluorescent protein genes in target cells. Nonetheless, the disadvantages of fluorogenic substrates and fluorescent proteins - limited diversity of available fluorophores and need for genetic transformation, respectively - could be circumvented if the microinjection of fluorescent probes would be possible without significant turgor-related artifacts.

Previously we had developed pico gauges for intracellular pressure measurements in all cell types, including very small and sensitive ones that had defied earlier attempts with conventional pressure microprobes (Knoblauch et al., 2014). The physical basis for pressure detection with pico gauges is the compression of nano- or picoliter volumes of silicon oil entrapped in micropipette tips. By reducing the fluid volume in the pipettes down to the volume range of typical cells, we were able to minimize artificial turgor shifts caused by fluid compressibility and by the pressure differential between micropipette and cell (Knoblauch et al., 2014). The successful application of pico gauges in testing the Münch hypothesis of phloem transport (Knoblauch et al., 2016b) suggested that similar methodological improvements might be achievable for microinjection techniques.

Here we describe the development and application of the diffusive injection micropipette (DIMP). The sources of several types of pressure artifacts are eliminated in DIMPs due to the reduced fluid volume in the pipette, which is in the range of or below the volume of the target cells. Injection proceeds by diffusion rather than pressure-driven flow. We report proof-of-principle experiments in plant, fungal, and animal cells, and demonstrate the method's potential for quantifying the diffusive transport in symplasmic cell arrays.

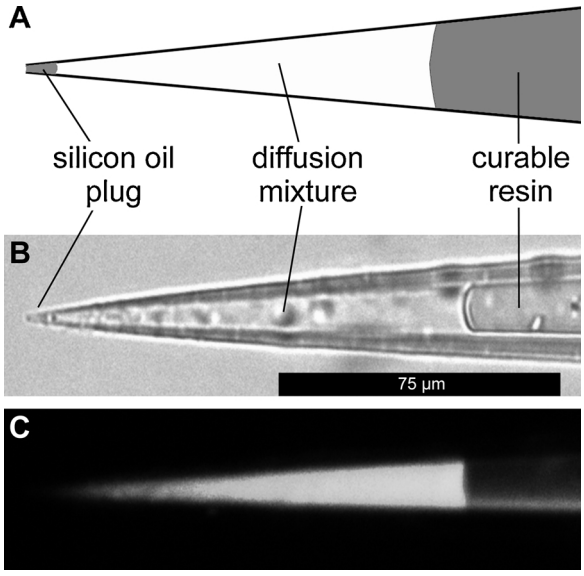

Fig. 1. Schematic drawing (A), brightfield micrograph (B), and fluorescence micrograph (C) of a ready-to-use diffusive injection micropipette (DIMP) filled with a Lucifer Yellow diffusion mixture.

2. Material and methods

2.1. DIMP production and application

Diffusive injection micropipettes (DIMPs) resemble pico gauges (Knoblauch et al., 2014) with certain modifications that create novel functionalities. DIMPs are characterized by the very small volume of the fluorophore solution that is to be introduced into a cell (Fig. 1). This diffusion mixture replaces the silicon oil that is used to monitor pressure changes in pico gauges. Knoblauch et al. (2014) had descibed two methods - 'A' and 'B'- for the production of pico gauges, both of which proved suitable for manufacturing DIMPs. Initially we applied method A to produce DIMPs with diffusion mixture volumes above 1 pL, and method B for DIMPs in the fL range. Since we were aiming at minimizing the fluid volume, and because we were able, with some practice, to manufacture about three times as many DIMPs per unit time by method B compared to method A, the former became our preferred standard procedure. In the following, we therefore describe method B in detail.

Micropipettes were made from B100-50-10 glass capillaries (i.d. 0.5 mm, o.d. 1.0 mm; Sutter Instrument, Novato CA, USA) using a Sutter model P-2000 micropipette puller. Pipettes with tip diameters ranging from 0.3 to 0.6 µm were used, depending on cell type. The pipettes were back-filled using custom-built microloaders with Loctite 352 (Henkel AG & Co, Düsseldorf, Germany), a UV-curable resin (Fig. 2 Step 1). The micropipette was then connected to a pressure manifold, mounted on a micromanipulation system, and brought into focus under a fluorescence microscope. Pressure of approximately 1 MPa was applied to the back end of the micropipette to drive the resin toward the pipette tip (Fig. 2 Step 2). Once the tip was filled, pipettes were lowered into a droplet of distilled water and pressure was reduced to ambient, so that water was driven into the pipette tip by capillary forces pushing back the resin. When the desired volume of water had filled the pipette,

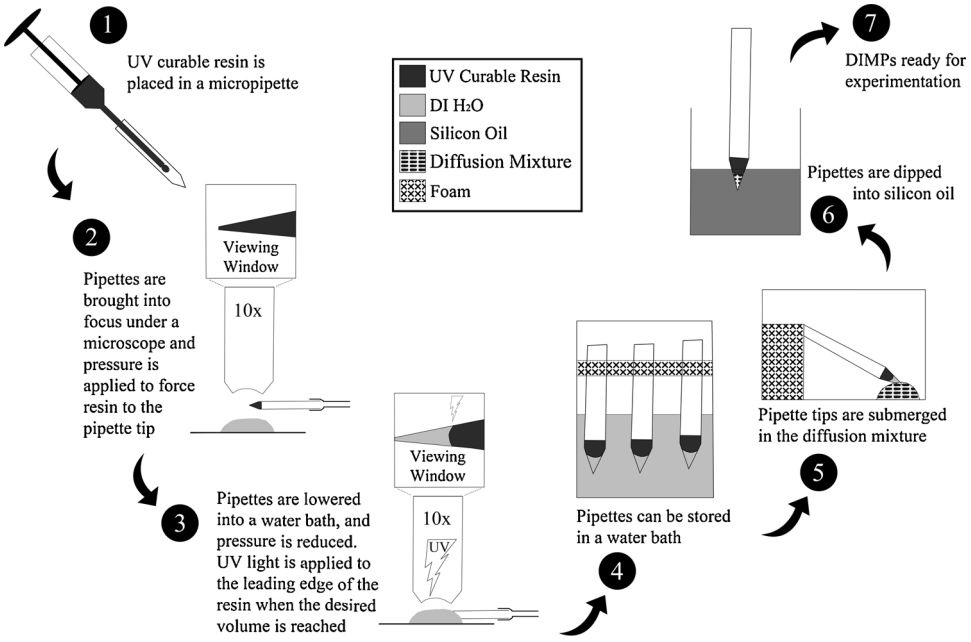

Fig. 2. Workflow for the production of DIMPs. See Materials and methods Section 2.1 for details.

UV light was applied to the leading edge of the water-resin interface to cure the resin (Fig. 2 Step 3). Alternatively, in cases in which capillary forces were insufficient to draw water into the pipette tip, UV light was applied behind the tip and the resulting curing induced shrinkage of the resin, simultaneously pulling a small volume of water into the tip. With some practice, desired tip volumes in the pL and fL range could reliably be produced. Micropipettes prepared to this stage were stored for prolonged periods (several months) with the tips submerged in distilled water that was replaced frequently to avoid contamination (Fig. 2 Step 4).

Diffusion mixtures consisted of 0.06 mM (in some experiments 0.05 mM) each of up to three different fluorophores in 100 mM KCl. In the experiments reported here, the Alexa Fluor dyes AF 488 (hydrazide sodium salt; size of the fluorescent anion: 547 Da), AF 568 (cadaverine diammonium salt; size of the fluorescent anion: 777 Da), and AF 633 (hydrazide bis-(triethyl-ammonium) salt; size of the fluorescent anion: 946 Da) were employed (Invitrogen Molecular Probes, Waltham MA, USA). To load the diffusion mixture, the prepared micropipettes were transferred to a custom-built foam holder and the tips were submerged in a droplet of the mixture for 30 min (Fig. 2 Step 5); larger pipettes may require longer periods to allow for diffusive equilibration of the fluorophore concentrations. Finally, the micropipettes were removed from the holder and their tips dipped into 50 cSt silicon oil (Sigma-Aldrich; MilliporeSigma, St. Louis MO, USA) for 3 s to produce an oil plug that sealed the tip and prevented evaporation from the diffusion mixture (Fig. 2 Step 6). DIMPs were used within 1 h after loading with the diffusion mixture and addition of the oil plug. To inject fluorophores, cells were impaled with DIMPs that then remained in place without further manipulations to allow for diffusion of fluorophores into the cytoplasm.

2.2. Pressure microinjection

Pressure microinjection probes were prepared as detailed by Oparka et al. (1991). The probes were mounted on a custom-made microinjection device as described in detail by Kempers et al. (1999). Before impalement, pipettes were pre-pressurized to the expected turgor of the cells.

2.3. Microscopy

All microinjection experiments were performed on the stage of a Leica TCS SP8 Confocal Laser-Scanning Microscope (CLSM) controlled with the Leica LAS X software (Leica Microsystems, Wetzlar, Germany). Various water-immersion and standard objectives were used as appropriate for different objects. The behavior of the injected fluorophores in the cells was documented by multichannel time-lapse photography (brightfield and up to three fluorescence channels) at 0.38 fps (2.6 s interval between photographs). All fluorescence micrographs presented in this paper are optical cross-sections.

2.4. Experimental organisms

Nicotiana tabacum plants were grown in a greenhouse at 23 °C, with 60–70% relative humidity and a 14/10-h light/dark period (daylight plus additional lamp light; 200 W full spectrum LED) and a minimum irradiance of 150 mmol m^{-2} s^{-1}. Leaves were excised with a new razor blade from non-flowering plants and the petioles were immediately submerged in Eppendorf vials with tap water. The adaxial surface was secured on the stage of the microscope with double sided tape. Trichome cells were impaled with DIMPs or pressure microinjection pipettes.

Aspergillus niger colonies provided by Taylor Bruchet and Tarah S. Sullivan (http://css.wsu.edu/tarah-s-sullivan/), WSU Department of Crop and Soil Sciences, were maintained on a 3% (w/v) agarose mixture (50% potato dextrose, 50% phytagel) at 25 °C in the dark.

Cultures of human prostate cancer cell lines LNCaP and PC-3 were provided by Brian S. Backer and Cliff Berkman (https://chem.wsu.edu/faculty/cliff-berkman/), WSU Department of Chemistry.

2.5. Image processing and analysis

Micrographs were processed with Image J (https://imagej.nih.gov/ij/), adhering to accepted rules for appropriate image manipulations (Blatt and Martin, 2013). Videos for publication were created with QuickTime 7 Pro (https://support.apple.com/quicktime).

Visualizations of time-courses of fluorescence intensity along trichomes and hyphae were generated from time-lapse micrograph series by treating the time-series as if they were z-stacks; application of the 3-

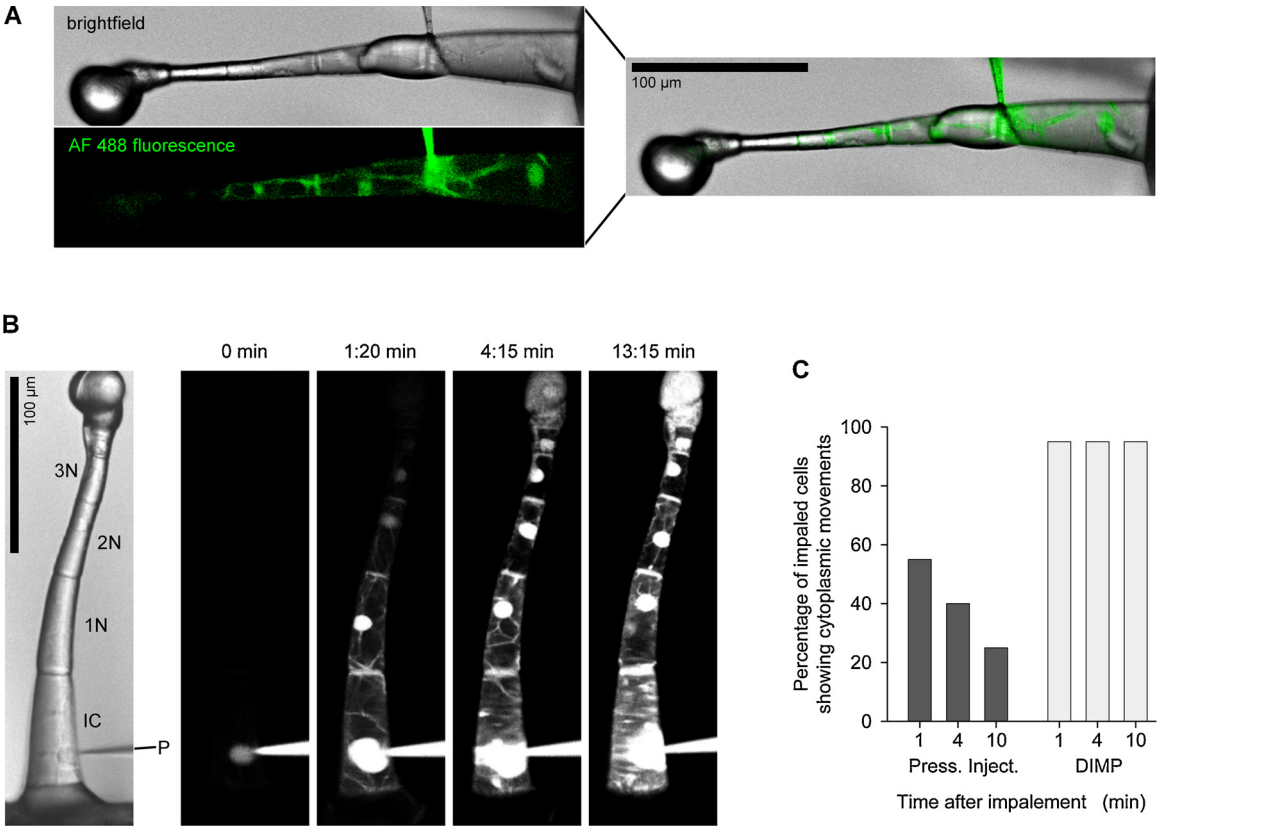

Fig. 3. Fluorophore introduction into cells of trichomes on *Nicotiana tabacum* leaves with DIMPs and by conventional pressure microinjection. A, diffusive injection of AF 488. The brightfield and fluorescence micrographs taken at 13 min after impalement demonstrate the localization of the stain in nuclei and transvacuolar cytoplasmic strands. The dynamics of the cytoplasmic strands are clearly seen in the corresponding video (Supplemental Video 1). B, pressure injection of AF 488. The brightfield image (left) shows the injection pipette (P) next to the injected cell (IC) just before impalement. The first, second, and third neighboring cells are marked (1N, 2N, and 3N, respectively). The four fluorescence micrographs (right) were taken at the times indicated on top following the start of pressure injection; time 0 is the first frame after impalement from a video sequence taken at 0.38 fps. At 1:20 min, mobile cytoplasmic strands are stained in IC and 1N. Three minutes later, these strands are mostly replaced by irregular speckles in IC but start to become visible in 2N. After 13:15 min, only remnants of strands remain in 1N, but branched strands are visible in 2N. Compare the corresponding video (Supplemental Video 3). C, percentages of trichome cells injected with AF 488 showing dynamic cytoplasmic strands at 1, 4, and 10 min after pressure injection compared to injection using DIMPs (n = 20 for each method).

D projection algorithm of ImageJ produced the time-courses presented as Figs. 4C,F and 5 C. In this analytical process, we applied an intensity threshold (20% of the maximum fluorescence intensity) to reduce unspecific background signal.

We compared the invasiveness of diffusive and pressure microinjection in *N. tabacum* trichomes using the breakdown of the transvacuolar strands as a criterion for the occurrence of adverse effects of the injection procedure. To exclude subjective bias, videos of the signal emitted from fluorophores in trichome cells (compare Supplemental Video 1) were blind-tested by colleagues who had not been involved in performing the experiments; the results in Fig. 3C came from these evaluators who did not know which type of method was shown in each video.

3. Results and discussion

3.1. DIMP design

Pico gauges are minimally invasive tools for measuring turgor pressure (Knoblauch et al., 2014). These micropipettes are mostly filled with a UV-curable glue, and after curing consist entirely of solid materials except for an nL or pL volume of silicon oil in the tip. After impalement of a turgescent cell, small changes of the volume of the oil can be monitored to determine the intracellular hydrostatic pressure (Knoblauch et al., 2014). Two modifications were made to the design of pico gauges to develop a minimally invasive system for the introduction of membrane-impermeant fluorophores into turgescent cells (Fig. 1). First, the silicon oil used in pico gauges was replaced by the diffusion mixture, an aqueous solution containing the fluorophore(s) that were to be introduced into the target cell (Figs. 1,2). Once a cell had been impaled by the DIMP, the diffusion mixture was in contact with the cytoplasm through the tip opening, and the fluorophore(s) could diffuse into the cell. An important difference between this technique on one hand and pressure microinjection and iontophoresis systems on the other is that no active regulation of hydrostatic pressure, electrical currents, or other physical or chemical parameters are required in DIMPs. No net volume changes occur between the impaled cell and the DIMP, since exchanges of molecules occur by diffusion alone. The final concentration of probes in the cell will depend on the diffusive equilibrium between the cytoplasm and the diffusion mixture in the DIMP, which can be controlled by adjusting the composition of the diffusion mixture when producing the DIMPs. Consequently, the equipment required by the DIMP methodology is comparatively simple and much less expensive than that needed for pressure microinjection and iontophoresis experiments.

The second modification was the addition of a small silicon oil plug at the very tip of the pipette (Figs. 1,2). This was necessary for two reasons. First, in initial attempts to produce DIMPs without oil plugs, we frequently observed evaporation from the diffusion mixture during handling of the pipettes, which led to the formation of gas pockets in the pipette tip. Second, without oil plugs, fluorescent dyes were observed diffusing out of the pipette tip while approaching the target cells

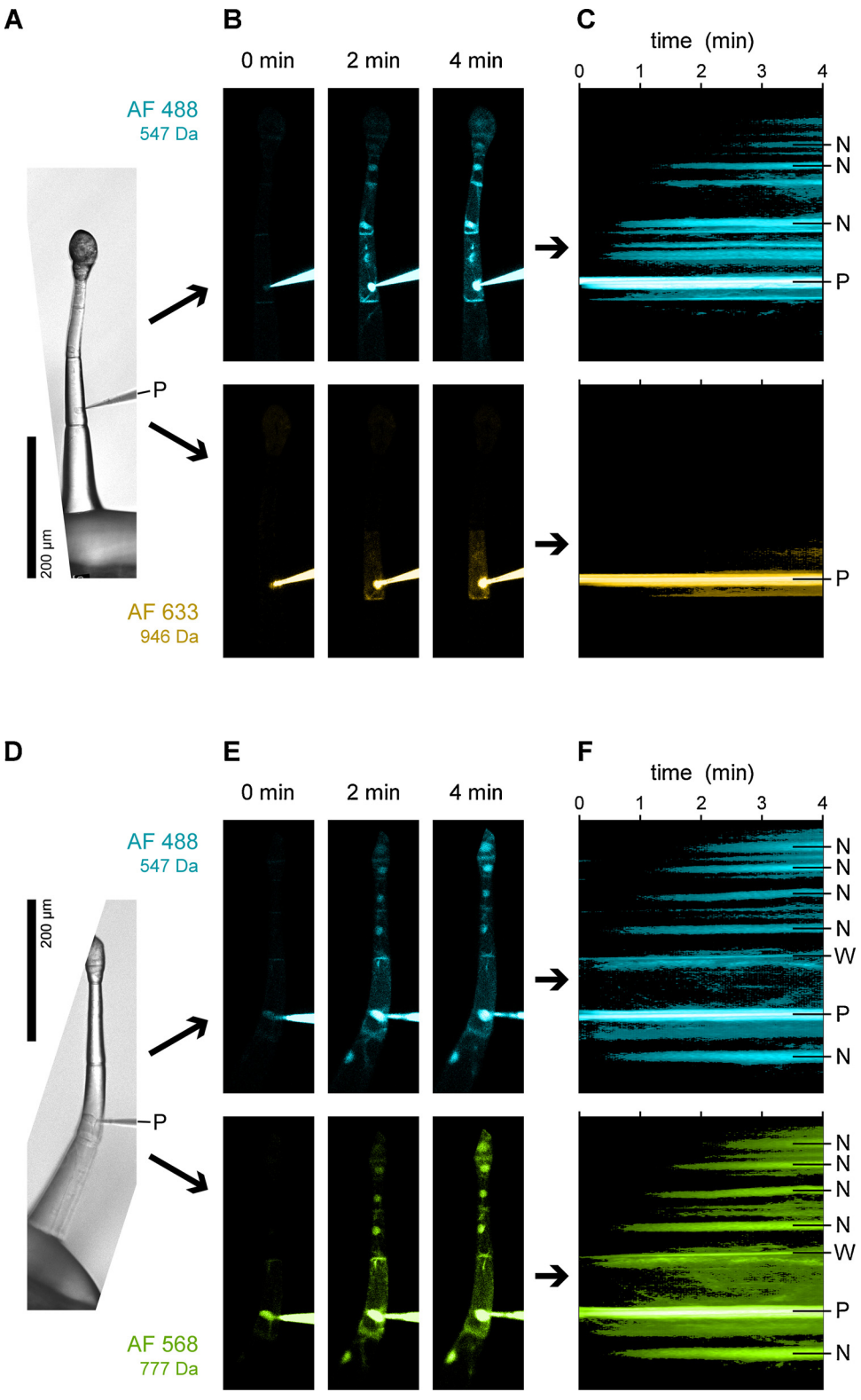

Fig. 4. Comparison of the movements of fluorescent dyes with different molecular masses applied pair-wise (AF 488 with AF 633 in A to C; AF 488 with AF 568 in D to F) to *Nicotiana tabacum* trichomes with DIMPs. A and D, brightfield images of the trichomes show the position of the micropipette (P). B and E, fluorescence micrographs selected from image series taken at 2.6 s intervals (0.38 fps) over 4 min; time after impalement indicated on top (time 0 is the first frame after impalement). C and F, z-projections of the image series, representing time-courses of the spread of fluorescence. A threshold of 20% of the signal intensity emitted from the micropipette was applied to reduce background noise. N, nucleus; P, micropipette; W, cross wall between cells.

under water immersion objectives. Silicon oil has been used as the standard filling of pressure microprobes for many decades (Tomos and Leigh, 1999) and does not seem to have negative effects on live plant cells. The oil plug usually moved back into the pipette when a cell was impaled by the DIMP, allowing the diffusion mixture to come into contact with the cytoplasm. Experiments in which this did not happen generally were discarded.

3.2. Testing DIMPs in Nicotiana tabacum trichomes and other plant cells

The epidermis of shoot organs of *Nicotiana* spp. develops glandular trichomes that consist of a more or less globular gland positioned on a uniseriate, multicellular stalk. This trichome stalk is a model system for studying symplasmic transport through plasmodesmata (Oparka and Prior, 1992; Waigmann and Zambryski, 2000; Christensen et al., 2009; Barton et al., 2011). We chose the trichomes of *N. tabacum* leaves to test

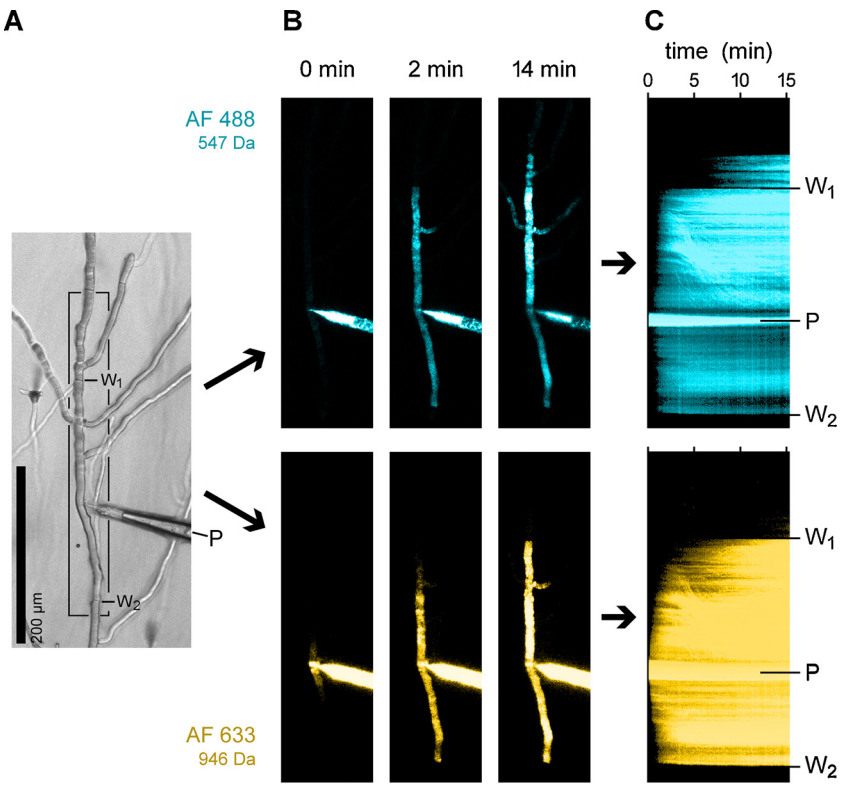

Fig. 5. Comparison of the movements of two fluorescent dyes with different molecular masses (AF 488 and AF 633) applied simultaneously to an *Aspergillus niger* hypha with a DIMP. A, brightfield micrograph of the branched hypha showing the position of the diffusion micropipette (P) and the two cross-walls (W_1, W_2) that confine the impaled cell. The distal direction (toward the hyphal tips) is upward. B, selected fluorescence micrographs from image series taken at 2.6 s intervals over a period of 16 min; time after impalement indicated on top (time 0 is the first frame after impalement). C, z-projections of the region marked by the black rectangle in A, covering the entire image series. These projections visualize the spread of fluorescence in the impaled hypha. To reduce background noise, a threshold of 20% of the signal intensity emitted from the micropipette was applied. P, micropipette; W_1 and W_2, cell walls also marked in A.

whether our newly designed DIMPs worked as intended. Impalement of the basal cells of trichome stalks with DIMPs loaded with an Alexa Fluor (AF) 488 solution resulted in rapid staining of the nucleus and the cytoplasm (Fig. 3A). The fluorescence signal appeared in the cell's apical neighbors with a delay that increased with increasing distance from the impaled cell (Supplemental Video 1). In over 90% of the experiments we conducted, no movement of the signal from the basal stalk cell into the subtending epidermal cells became evident. In the remaining cases, weak AF 488 fluorescence was detected in epidermal cells. These findings corroborated earlier work using different fluorophores, that had implied preferentially unidirectional transport through plasmodesmata at the epidermis/trichome interface (Christensen et al., 2009).

We also applied DIMP injection successfully to an arbitrary selection of plant cells available in our lab, including guard cells of *N. tabacum*, pavement and mesophyll cells of *Ipomea nil* and *Populus trichocarpa*, and the green alga *Spirogyra* sp. (not shown). Taken together, these results demonstrated the practical feasibility of diffusive microinjection.

3.3. DIMPs vs conventional pressure injection

The large central vacuoles of numerous cell types in plants are traversed by transvacuolar strands, cytoplasmic links connecting distant cytoplasmic regions (Oda et al., 2009). Transvacuolar strands are formed around robust actin filament bundles that enable particularly fast transport of organelles and cytoplasmic streaming (Thomas et al., 2009). The strands themselves are highly dynamic, continuously changing their arrangement and branching pattern in vigorous cells (Hoffmann and Nebenführ, 2004). Several of the fluorescent dyes we introduced into *N. tabacum* trichome cells using DIMPs, for example AF 488, remained restricted to the nuclei and cytoplasm. This facilitated the observation of the dynamics of transvacuolar strands, which are highly active in these cells. As a rule, we observed movement and continuous reorganization of the strands throughout the duration of the experiments (20 min in the example presented as Fig. 3A and Supplemental Video 1). This indicated that the dynamic, cytoskeleton-dependent mechanisms by which the cells control their internal organization were mostly unaffected by the diffusive microinjection with DIMPs.

The situation was different when we introduced the dyes by pressure microinjection. At first sight, similar results were obtained: the fluorescence signal distributed from the impaled basal stalk cell towards the apical gland over a time scale of minutes. We frequently observed, however, a replacement of the coordinated movement of the transvacuolar strands in the impaled cell by a random wobbling of irregularly distributed foci, apparently Brownian motion of small portions of cytoplasm. Such loss of intracellular organization occurred immediately after impalement (Supplemental Video 2) or after some time (Fig. 3B; Supplemental Video 3). In one third of the cases in which the phenomenon was observed in the impaled cell, it also occurred in the neighboring cell, with a delay (Fig. 3B; Supplemental Video 3).

We had recorded 20 pressure microinjections of AF 488 or AF 568 into basal trichome cells before we became aware of the effects on the intracellular organization in some of the experiments. This unawareness probably occurred, first, because the expected result, namely the slow expansion of the fluorescence signal from the trichome's base to its apex, always could be observed; and second, because no fluorescence signal was detected extracellularly, which usually is understood to imply a successful, stable impalement. However, subsequent analysis of the videos showed that in almost half of the apparently successful pressure injection experiments, the coordinated movements of the transvacuolar strands had ceased before 1 min after impalement (Fig. 3C). The proportion of impaled cells showing their normal behavior further decreased to 25% at 10 min after impalement. In contrast, in the 20 analogous experiments conducted with DIMPs, no obvious changes in the cytoplasmic dynamics of any cell were evident after 10 min in 19 (95%) cases (Fig. 3C). These results suggested that diffusive microinjection caused a breakdown of the intracellular organization of the impaled cells in a significantly lower proportion of the experiments than pressure microinjection did.

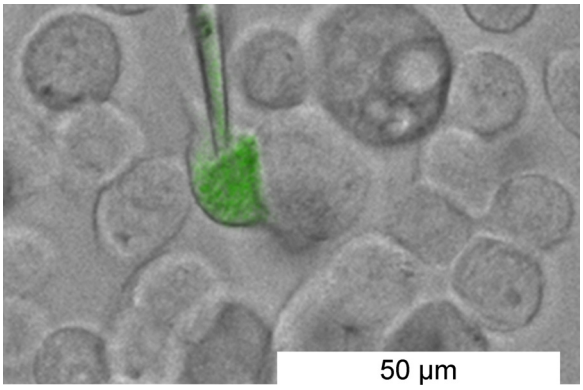

Fig. 6. Diffusive injection of AF 568 (rendered green) into an individual cell in a PC3 human prostate cancer cell culture. The image is an overlay of the brightfield and the corresponding fluorescence micrographs taken 3 min after impalement.

3.4. Simultaneous injection of multiple fluorophores

We injected pairs of Alexa Fluor dyes differing in molecular size into the second cell of trichome stalks and followed their movement along the cell file. The relatively small AF 488 (547 Da) moved quickly out of the impaled cell in the apical direction whereas the 73% heavier, simultaneously applied AF 633 (946 Da) did not (Fig. 4A-C; Supplemental Video 4). When we applied AF 488 combined with the only 42% heavier AF 568 (777 Da), we observed similar behavior of the two fluorophores although AF 568 moved slightly slower (Fig. 4D-F). These results obviously agreed with the general expectation that smaller molecules should diffuse faster than larger ones. Further quantitative evaluations would seem overly speculative at this time, as diffusion coefficients for the various derivatives of AF fluorophores are mostly unavailable or differ significantly between published studies (e.g. for AF 488 in pure water at 25°: 430 $\mu m^2 s^{-1}$[Nitsche et al., 2004], 414 $\mu m^2 s^{-1}$ [Petrov et al., 2006], and 457 $\mu m^2 s^{-1}$ [Petrášek and Schwille, 2008]).

As an intriguing detail, significant movement of the fluorescence signal(s) towards the base of the trichome occurred in some experiments (for instance, Fig. 4D-F) but less so in others (Fig. 4A-C). Together with our observation that fluorophores always traveled into more apical cells when injected into the basal trichome cell (Fig. 3), this result pointed to a regulated directionality of cell-to-cell transport through plasmodesmata. The phenomenon calls for further study, as Christensen et al. (2009) had described transport directionality in trichomes, but only at the epidermis-trichome interface. Concerning our methodology, we concluded that the composition of the diffusion mixture in the tip of a DIMP may be complex, and that the number of fluorophores that usefully can be applied in combination rather is limited by the microscope's capacity for the simultaneous monitoring of multiple channels.

3.5. DIMPs applied to fungal hyphae

Microinjection of fungal cells and especially hyphae is a potentially powerful experimental tool, but it appears somewhat underused (Jackson, 1995). This may be due to impalement-induced artifacts including the - sometimes transient - stoppage of cytoplasmic streaming and hyphal tip growth (Jackson, 1995). We used the euascomycete *Aspergillus niger* to test whether the DIMP method can be applied successfully to hyphal cells. Diffusive injection worked as it did in plant cells, and yielded some unexpected results. When fluorescent dyes diffused into the impaled cell, their movement sometimes stopped at one or both of the septa separating the cell from its neighbors, and sometimes not. In the example presented as Fig. 5, the applied fluorophores, AF 488 and AF 633, initially remained contained in the impaled cell and did not cross over the distal and proximal cell boundaries (W_1 and W_2, respectively, in the figure). At around 7 min after impalement, however, W_1 opened for AF 488 but not for the 73% heavier molecules of AF 633 (Fig. 5C), while W_2 stayed closed. The AF 488 signal appeared almost simultaneously along the length of the cell distal of W_1 (Fig. 5C), indicating that diffusion and/or cytoplasmic streaming was far too rapid to account for the delay of AF 488 movement into this cell. While the observations we have collected so far do not yet justify the suggestion of a hypothetical mechanism, we conclude that the septal pores in the cross-walls of the hyphae of *A. niger* are regulated in a complex fashion. This conclusion is in line with current ideas about long-distance transport and its regulation in the symplasmic hyphal network of *A. niger* and of euascomycetes in general (Bleichrodt et al., 2012; Shen et al., 2014). We expect that DIMPs will prove a valuable tool in further expanding our understanding of the underlying mechanisms.

3.6. DIMPs applied to animal cells

Finally we were interested to see whether DIMPs, which we had designed for microinjection into turgescent cells while minimizing turgor-dependent artifacts, were applicable to wall-less cells that lack significant intracellular pressure. We introduced AF 568 via diffusive injection into human prostate cancer cells of the cultured lines LNCaP (Horoszewicz et al., 1983) and PC3 (Kaighn et al., 1979). The intensity of the fluorescence signals within the cells reached plateaus (saturation) after 3–5 min, and no spreading of the signal to neighboring cells was observed (Fig. 6; it should be noted that the size of AF 568, 777 Da, is in the range of the apparent size exclusion limit of most gap junctions; Weber et al., 2004). We concluded that diffusive microinjection works well not only in walled cells of plants and fungi, but also in wall-less animal cells, suggesting that it can be applied also to isolated plant cell protoplasts.

4. Conclusion

Fluid-filled pipettes for microinjection of materials into turgescent live cells potentially disturb the intracellular hydrostatic pressure through three mechanisms: (1) leakage at the insertion point, (2) fluxes of cytoplasm or pipette filling into or out of the pipette due to pressure differentials between the interior of the cell and the pipette, and (3) compressibility effects in the comparatively large volume of the pipette system. We designed a novel type of micropipette with the aim of eliminating mechanisms (2) and (3), by bringing the volume of the pipette filling down into the range of typical cell sizes. Moreover, we simplified the experimental setup by utilizing the least invasive mode of 'injection': diffusion. This avoided the necessity for actively regulating pressure or electrical currents as required for pressure microinjection and iontophoresis, respectively. It also excluded the possibility of artifacts caused by pressure and electrical pulses in the injected cells.

Our experiments carried out with plant (Figs. 3,4), fungal (Fig. 5), and wall-less animal cells (Fig. 6) demonstrate that our diffusive injection micropipettes, or DIMPs, work as expected - but do they establish a methodological improvement over standard techniques such as pressure microinjection? It is next to impossible to evaluate the efficiencies of microinjection techniques based on the published literature since success rates of impalement attempts are hardly ever quantified. We performed pressure as well as diffusive microinjection on cells of *N. tabacum* trichomes, and observed the dynamics of transvacuolar strands as a criterion for the healthiness of the impaled cells. Based on the continuous presence of dynamic strands over a period of 10 min following impalement, our results suggest an almost four-fold increased success rate of DIMPs compared to pressure-injection micropipettes (Fig. 3C). This finding inspires confidence in DIMPs as the least invasive microinjection methodology that is available at this time.

Declarations of Competing Interests

None.

Acknowledgments

We are indebted to Brian S. Backer and Cliff Berkman for providing cultures of prostate cancer cells, Taylor Bruchet and Tarah S. Sullivan for providing *Aspergillus niger* colonies, and Jan Knoblauch for help in analyzing data. We thank the Franceschi Microscopy and Imaging Center at Washington State University (https://sbs.wsu.edu/facilities/franceschi-microscopy-imaging-center/) for technical support, and two anonymous reviewers for constructive criticism of an earlier version of the manuscript. This work was supported by the US National Science Foundation (grant number 1656769).

Appendix A. Supplementary data

Supplementary material related to this article can be found, in the online version, at https://doi.org/10.1016/j.jplph.2019.153060.

References

Adam, V., 2014. Phototransformable fluorescent proteins: which one for which application? Histochem. Cell Biol. 142, 19–41.
Baron-Epel, O., Hernandez, D., Jiang, L.W., Meiners, S., Schindler, M., 1988. Dynamic continuity of cytoplasmic and membrane compartments between plant cells. J. Cell Biol. 106, 715–721.
Barton, D.A., Cole, L., Collings, D.A., Liu, D.Y.T., Smith, P.M.C., Day, D.A., Overall, R.L., 2011. Cell-to-cell transport via the lumen of the endoplasmic reticulum. Plant J. 66, 806–817.
Blatt, M., Martin, C., 2013. Manipulation and misconduct in the handling of image data. Plant Physiol. 163, 3–4.
Bleichrodt, R.J., van Veluw, G.J., Recte, B., Maruyama, J., Kitamoto, K., Wösten, H.A.B., 2012. Hyphal heterogeneity in *Aspergillus oryzae* is the result of dynamic closure of septa by Woronin bodies. Mol. Microbiol. 86, 1334–1344.
Brandizzi, F., Fricker, M., Hawes, C., 2002. A greener world: the revolution in plant bioimaging. Nat. Rev. Mol. Cell Biol. 3, 520–530.
Christensen, N.M., Faulkner, C., Oparka, K., 2009. Evidence for unidirectional flow through plasmodesmata. Plant Physiol. 150, 96–104.
Enterina, J.R., Wu, L., Campbell, R.E., 2015. Emerging fluorescent protein technologies. Curr. Op. Chem. Biol. 27, 10–17.
Green, P.B., 1968. Growth physics in *Nitella*: a method for continuous in vivo analysis of extensibility based on a micro-manometer technique for turgor pressure. Plant Physiol. 43, 1169–1184.
Hoffmann, A., Nebenführ, A., 2004. Dynamic rearrangements of transvacuolar strands in BY-2 cells imply a role of myosin in remodeling the plant actin cytoskeleton. Protoplasma 224, 201–210.
Horoszewicz, J.S., Leong, S.S., Kawinski, E., Karr, J.P., Rosenthal, H., Chu, T.M., Mirand, E.A., Murphy, G.P., 1983. LNCaP model of human prostatic carcinoma. Cancer Res. 43, 1809–1818.
Jackson, S.L., 1995. Microinjection of fungal cells: a powerful experimental technique. Can. J. Bot. 73 (Suppl. 1), S435–S443.
Kaighn, M.E., Narayan, K.S., Ohnuki, Y., Lechner, J.F., Jones, L.W., 1979. Establishment and characterization of a human prostatic carcinoma cell line (PC-3). Invest. Urol. 17, 16–32.
Kempers, R., van Bel, A.J.E., 1997. Symplasmic connections between sieve element and companion cell in the stem phloem of *Vicia faba* L. have a molecular exclusion limit of at least 10 kDa. Planta 201, 195–201.
Kempers, R., Prior, D.A.M., Oparka, K.J., Knoblauch, M., van Bel, A.J.E., 1999. Integration of controlled intracellular pressure microinjection, iontophoresis, and membrane potential measurement. Plant Biol. 1, 61–67.
Knoblauch, J., Mullendore, D.L., Jensen, K.H., Knoblauch, M., 2014. Pico gauges for minimally invasive intracellular hydrostatic pressure measurements. Plant Physiol. 166, 1271–1279.
Knoblauch, J., Peters, W.S., Knoblauch, M., 2016a. The gelatinous extracellular matrix facilitates transport studies in kelp: visualization of pressure-induced flow reversal across sieve plates. Ann. Bot. 117, 599–606.
Knoblauch, M., 2001. Microinjection. In: Hawes, C., Satiat-Jeunemaitre, B. (Eds.), Plant Cell Biology. A Practical Approach, 2nd ed. Oxford University Press, Oxford, pp. 134–157.
Knoblauch, M., Knoblauch, J., Mullendore, D.L., Savage, J.A., Babst, B.A., Beecher, S.D., Dodgen, A.C., Jensen, K.H., Holbrook, N.M., 2016b. Testing the Münch hypothesis of long distance phloem transport in plants. eLife 5, e15341.
Knoblauch, M., van Bel, A.J.E., 1998. Sieve tubes in action. Plant Cell 10, 35–50.
Lucas, W.J., Lee, J.Y., 2004. Plasmodesmata as a supracellular control network in plants. Nat. Rev. Mol. Cell Biol. 5, 712–726.
Martens, H.J., Hansen, M., Schulz, A., 2004. Caged probes: a novel tool in studying symplasmic transport in plant tissue. Protoplasma 223, 63–66.
Maruyama, J., Juvvadi, P.R., Ishi, K., Kitamoto, K., 2005. Three-dimensional image analysis of plugging at the septal pore by Woronin body during hypotonic shock inducing hyphal tip bursting in the filamentous fungus *Aspergillus oryzae*. Biochem. Biophys. Res. Comm. 331, 1081–1088.
Mitchison, T.J., Sawin, K.E., Theriot, J.A., Gee, K., Mallavarapu, A., 1998. Caged fluorescent probes. Meth. Enzymol. 291, 63–78.
Nitsche, J.M., Chang, H.-C., Weber, P.A., Nicholson, B.J., 2004. A transient diffusion model yields unitary gap junctional permeabilities from images of cell-to-cell fluorescent dye transfer between *Xenopus* oocytes. Biophys. J. 86, 2058–2077.
Oda, Y., Higaki, T., Hasezawa, S., Kutsuna, N., 2009. New insights into plant vacuolar structure and dynamics. Intern. Rev. Cell Mol. Biol. 277, 103–135.
Oparka, K.J., Boevink, P., 2005. Techniques for imaging intercellular transport. In: Oparka, K.J. (Ed.), Plasmodesmata. Blackwell, Oxford, pp. 241–262.
Oparka, K.J., Duckett, C.M., Prior, D.A.M., Fisher, D.B., 1994. Real-time imaging of phloem-unloading in the root tip of *Arabidopsis*. Plant J. 6, 759–766.
Oparka, K.J., Murphy, R., Derrick, P.M., Prior, D.A.M., Smith, J.A.C., 1991. Modification of the pressure-probe technique permits controlled intracellular microinjection of fluorescent probes. J. Cell. Sci. 98, 539–544.
Oparka, K.J., Prior, D.A.M., 1992. Direct evidence for pressure-generated closure of plasmodesmata. Plant J. 2, 741–750.
Petrášek, Z., Schwille, P., 2008. Precise measurement of diffusion coefficients using scanning fluorescence correlation spectroscopy. Biophys. J. 94, 1437–1448.
Petrov, E.P., Ohrt, T., Winkler, R.G., Schwille, P., 2006. Diffusion and segmental dynamics of double-stranded DNA. Phys. Rev. Lett. 97, 258101.
Radford, J.E., White, R.G., 2001. Effects of tissue-preparation-induced callose synthesis on estimates of plasmodesma size exclusion limits. Protoplasma 216, 47–55.
Rodriguez, E.A., Campbell, R.E., Lin, J.Y., Lin, M.Z., Miyawaki, A., Palmer, A.E., Shu, X., Zhang, J., Tsien, R.Y., 2017. The growing and glowing toolbox of fluorescent photoactive proteins. Trends Biochem. Sci. 42, 111–129.
Ross-Elliott, J., Jensen, K.H., Haaning, K.S., Wager, B.M., Knoblauch, J., Howell, A.H., Mullendore, D.L., Monteith, A.G., Paultre, D., Yan, D., Otero, S., Bourdon, M., Sager, R., Lee, J.Y., Helariutta, Y., Knoblauch, M., Oparka, K.J., 2017. Phloem unloading in *Arabidopsis* roots is convective and regulated by the phloem-pole pericycle. eLife 6, e24125.
Rutschow, H.L., Baskin, T.I., Kramer, E.M., 2011. Regulation of solute flux through plasmodesmata in the root meristem. Plant Physiol. 155, 1817–1826.
Sanderson, M.J., Smith, I., Parker, I., Bootman, M.D., 2014. Fluorescence microscopy. Cold Spring Harb. Protoc. https://doi.org/10.1101/pdb.top071795.
Sanford, L., Palmer, A., 2017. Recent advances in development of genetically encoded fluorescent sensors. Meth. Enzymol. 589, 1–49.
Shen, K.F., Osmani, A.H., Govindaraghavan, M., Osmani, S.A., 2014. Mitotic regulation of fungal cell-to-cell connectivity through septal pores involves the NIMA kinase. Mol. Biol. Cell 25, 763–775.
Stockert, J.C., Blázquez-Castro, A., 2017. Fluorescence Microscopy in Life Sciences. Bentham eBooks, Sharjah.
Storms, M.M.H., van der Schoot, C., Prins, M., Kormelink, R., van Lent, J.W.M., Goldbach, R.W., 1998. A comparison of two methods of microinjection for assessing altered plasmodesmal gating in tissues expressing viral movement proteins. Plant J. 13, 131–140.
Thomas, C., Tholl, S., Moes, D., Dieterle, M., Papuga, J., Moreau, F., Steinmetz, A., 2009. Actin bundling in plants. Cell Motil. Cytoskel. 66, 940–957.
Tomos, A.D., Leigh, R.A., 1999. The pressure probe: a versatile tool in plant cell physiology. Plant Physiol. 50, 447–472.
Waigmann, E., Zambryski, P., 2000. Trichome plasmodesmata: a model system for cell-to-cell movement. Adv. Bot. Res. 31, 261–283.
Walia, A., Waadt, R., Jones, A.M., 2018. Genetically encoded biosensors in plants: pathways to discovery. Ann. Rev. Plant Biol. 69, 497–524.
Weber, P.A., Chang, H.-C., Spaeth, K.E., Nitsche, J.M., Nicholson, B.J., 2004. The permeability of gap junction channels to probes of different size is dependent on connexin composition and permeant-pore affinities. Biophys. J. 87, 958–973.
Wright, K.M., Horobin, R.W., Oparka, K.J., 1996. Phloem mobility of fluorescent xenobiotics in *Arabidopsis* in relation to their physicochemical properties. J. Exp. Bot. 47, 1779–1787.
Wright, K.M., Oparka, K.J., 1996. The fluorescent probe HPTS as a phloem-mobile, symplastic tracer: an evaluation using confocal laser scanning microscopy. J. Exp. Bot. 47, 439–445.
Zimmermann, U., Steudle, E., 1979. Physical aspects of water relations of plant cells. Adv. Bot. Res. 6, 45–117.